EMITTER International Journal of Engineering Technology
Vol. 12, No. 2, December 2024, pp. 112~127
DOI : 10.24003/emitter.v12i2.885

From Waste to Power: Fly Ash-Based Silicone Anode Lithium-Ion Batteries Enhancing PV Systems

Kania Yusriani Amalia[1], Tresna Dewi[2], Rusdianasari[3]

[1]Applied Master of Renewable Energy Engineering, Politeknik Negeri Sriwijaya, Jalan Srijaya Negara, Palembang, Indonesia
[2]Department of Electrical Engineering, Politeknik Negeri Sriwijaya, Jalan Srijaya Negara, Palembang, Indonesia
[3]Department of Renewable Energy Engineering, Politeknik Negeri Sriwijaya, Jalan Srijaya Negara, Palembang, Indonesia
Corresponding Author: tresna_dewi@polsri.ac.id

Received August 30, 2024; Revised October 5, 2024; Accepted November 18, 2024

Abstract

Indonesia's high solar irradiance, averaging 4.8 kWh/m^2/day, presents a significant opportunity to harness solar power to meet growing energy demands. Fly ash, abundant in Indonesia and rich in silicon dioxide (40-60% SiO_2), can be repurposed into high-value silicon anodes. The successful extraction of silicon from fly ash, increasing SiO_2 content from 49.21% to 93.52%, demonstrates the potential for converting industrial waste into valuable battery components. Combining these advanced batteries with PV systems improves overall efficiency and reliability. Energy charge and discharge experiments reveal high energy efficiency for silicon-anode batteries, peaking at 80.53% and declining to 67.67% after ten cycles. Impedance spectroscopy tests indicate that the S120 sample, with the lowest impedance values, is most suitable for high-efficiency applications. Photovoltaic (PV) system integration experiments show that while increased irradiance generally boosts power output, other factors like PV cell characteristics and load conditions also play crucial roles. In summary, leveraging Indonesia's solar potential with fly ash-based silicon anode batteries and advanced predictive analytics addresses energy and environmental challenges. This innovative approach enhances battery performance and promotes the circular economy by converting waste into high-value products, paving the way for a sustainable and efficient energy future.

Keywords: Energy Storage, IES, PV system, Renewable Energy, Silicon-anode Li-ion.

1. INTRODUCTION

Solar energy holds immense importance for Indonesia, offering a sustainable and reliable solution to meet the country's growing energy needs[1][2]. With its high solar irradiance levels, Indonesia is well-positioned to harness solar power to drive economic growth, enhance energy security,

reduce environmental impact, and support rural electrification[4][5][6]. Realizing this potential requires concerted efforts from the government, private sector, and local communities to create a conducive environment for solar energy development. By embracing solar power, Indonesia can pave the way for a greener, more sustainable future and set an example for other nations in the region, such as to transform automatic farming by providing a sustainable, cost-efficient, and reliable power source for various automated systems[7][8][9][10].

The quest for sustainable energy solutions is driving significant advancements in the integration of photovoltaic (PV) systems with cutting-edge energy storage technologies[11][12]. Among these, lithium-ion batteries (LIBs) stand out due to their high energy density, long cycle life, and efficiency[13][14][15]. However, the environmental impact of traditional battery materials and the necessity for improved performance necessitate the exploration of alternative, sustainable materials. Fly ash, a byproduct of coal combustion, has emerged as a promising candidate for this purpose[16][17][18][19][20].

Fly ash is primarily composed of silicon dioxide (SiO_2), aluminum oxide (Al2O3), and other trace elements, which contribute to its utility in various industrial applications[16][17][18][19][20][21]. Traditionally regarded as an industrial waste requiring costly disposal, fly ash contains a rich array of minerals and compounds that can be repurposed into valuable resources for battery technology. Recent research has focused on the use of fly ash to develop silicon anodes for LIBs, revealing significant improvements in battery performance and environmental sustainability.

Recent studies have demonstrated that the unique properties of fly ash, such as its high silicon content and porous structure, contribute to enhanced electrochemical performance when used in anode materials[14][21][22]. For instance, Shigemoto et al. (1993) explored the selective formation of Na-X zeolite from coal fly ash, highlighting the material's potential for high-value applications[19]. Similarly, Bukhari et al. (2015) reviewed the conversion of coal fly ash to zeolite utilizing microwave and ultrasound energies, emphasizing the material's versatility[20].

This paper investigates the transformative potential of fly ash-based silicon anode lithium-ion batteries and their role in enhancing the efficiency and sustainability of PV systems. By converting industrial waste into high-performance battery components, this approach addresses both environmental and technological challenges[23]. The principles of the circular economy are exemplified in this process, turning waste materials into high-value products and promoting sustainable development. This article explores the development and potential of fly ash-based silicone anode lithium-ion batteries for enhancing PV systems. This study is the pilot project; hence, focus more on the feasibility of implementing the idea of intersecting the material science and machine learning, this study highlights the transformative impact of these technologies on sustainable energy solutions

2. RELATED WORKS

The utilization of coal fly ash in various industrial applications has garnered significant attention due to its potential environmental and economic benefits. This article presents the transformation of coal fly ash into valuable materials, focusing on the feasibility of developing silicon-based anodes for lithium-ion batteries (LIBs) and its implications for enhancing PV systems.

Fly ash, a byproduct of coal combustion, has been extensively studied for its potential conversion into valuable materials. Shigemoto, Hayashi, and Miyaura (1993)[19] explored the selective formation of Na-X zeolite from coal fly ash using sodium hydroxide fusion prior to hydrothermal reaction. Their research demonstrated the feasibility of converting fly ash into zeolites, which have numerous industrial applications. Similarly, Bukhari et al. (2015)[20] reviewed the conversion of coal fly ash to zeolite utilizing microwave and ultrasound energies, highlighting the efficiency and environmental benefits of these methods.

Recent advancements have focused on the use of fly ash-derived silicon in LIB anodes. Silicon-based anodes offer a high theoretical capacity but face challenges related to volume expansion during lithiation. Jiang et al. (2017)[18] developed a sustainable route from fly ash to silicon nanorods, demonstrating their high performance in lithium-ion batteries. Liu et al. (2017)[17] synthesized silica-derived hydrophobic colloidal nano-Si for lithium-ion batteries, showcasing improved electrochemical performance. These studies highlight the potential of fly ash-derived silicon in enhancing battery performance and sustainability.

The integration of advanced lithium-ion batteries into PV systems can significantly enhance their efficiency and reliability. Dunn, Kamath, and Tarascon (2011) discussed the critical role of electrical energy storage for the grid, emphasizing the importance of advanced batteries[13]. Liu et al. (2015) explored the use of natural materials in battery anodes, demonstrating a sustainable approach to energy storage[17]. These advancements in battery technology are crucial for improving the performance of PV systems and ensuring a stable energy supply.

This study realizes the possibility of implementing the silicon anode lithium-ion battery from fly ash, which is environmentally beneficial. Repurposing industrial waste, such as fly ash, for battery materials can reduce the environmental impact of both coal combustion and battery production.

3. ORIGINALITY

The originality of this research lies in the innovative integration of coal fly ash-derived silicon-based anodes into lithium-ion batteries (LIBs) and their feasiblity of application in enhancing PV systems. This approach addresses multiple critical challenges in energy storage, waste management, and renewable energy integration, presenting a sustainable solution with

significant environmental and economic benefits. This study offers a novel pathway for utilizing industrial waste in high-value applications, thus contributing to a circular economy.

The most groundbreaking aspect of this research is the development of silicon-based anodes from fly ash for use in LIBs. Traditional silicon anodes face significant challenges related to volume expansion during lithiation, which affects battery performance and lifespan. Jiang et al. (2017) presented a sustainable route to convert fly ash into silicon nanorods, which showed high performance in lithium-ion batteries. Similarly, Liu et al. (2017) synthesized silica-derived hydrophobic colloidal nano-Si, demonstrating its superior electrochemical properties[17]. These studies provide a strong foundation for the development of fly ash-derived silicon anodes, highlighting their potential to revolutionize energy storage technologies.

The integration of advanced LIBs into PV systems can significantly enhance their efficiency and reliability, addressing the intermittency of solar energy. Dunn, Kamath, and Tarascon (2011) emphasized the critical role of advanced energy storage systems in supporting renewable energy integration[13]. By developing silicon-based anodes from fly ash, this research not only provides a sustainable solution for LIBs but also enhances the performance of PV systems. This dual benefit underscores the originality and potential impact of the proposed approach.

The originality of this research lies in its innovative approach to converting coal fly ash into silicon-based anodes for LIBs and integrating them into PV systems. This study offers a comprehensive solution with significant environmental and economic benefits by addressing critical challenges in waste management, energy storage, and renewable energy integration. The novel use of fly ash in high-value applications highlights the potential for sustainable development and the transition to a circular economy.

4. SYSTEM DESIGN

Fly ash, a byproduct of coal combustion, contains 40-60% silicon dioxide (SiO_2), 20-30% aluminum oxide (Al_2O_3), 5-10% iron oxide (Fe2O3), 1-10% calcium oxide (CaO), and smaller amounts of magnesium oxide (MgO), sulfate (SO_3), potassium oxide (K_2O), sodium oxide (Na_2O), titanium dioxide (TiO_2), and trace elements like phosphorus pentoxide (P_2O_5), manganese oxide (MnO), boron oxide (B_2O_3), strontium oxide (SrO), zinc oxide (ZnO), copper oxide (CuO), and chromium oxide (Cr_2O_3) each typically constitute less than 1%. Its composition makes it ideal for producing silicon nanoparticles for energy storage.

Figure 1 illustrates the process of converting fly ash into silicon nanoparticles for lithium-ion battery anodes. It begins with fly ash undergoing pre-treatment with sodium hydroxide (NaOH), creating fused fly ash through high-temperature fusion. The fused fly ash is then subjected to hydrochloric acid (HCl) leaching to remove aluminum and iron oxides, yielding high-purity silica. Next, the purified silica is mixed with magnesium (Mg) in a high-

temperature furnace, reducing silica (SiO_2) to elemental silicon (Si). Post-treatment processes like milling and classification produce uniform nanoscale silicon particles. The final products, Nano SiO_2 and MgO + Nano Si, are ready for use in battery anodes. This process increases the energy density of lithium-ion batteries, as silicon anodes have a much higher capacity than graphite, resulting in longer battery life and greater range for electric vehicles.

Figure 1. The process of extracting silicon Si from fly ash**.**

4.1 Battery Charging and Discharging Process

Figure 2 show the battery design process, where Figure 2 illustrates the functioning of an electrochemical cell (electron and ion flow during charging and discharging), inlcuding the anode (where oxidation occurs), the cathode (where reduction occurs), the electrolyte (allowing ion flow between electrodes), and the external circuit (connecting the anode and cathode outside the electrolyte for electron flow).

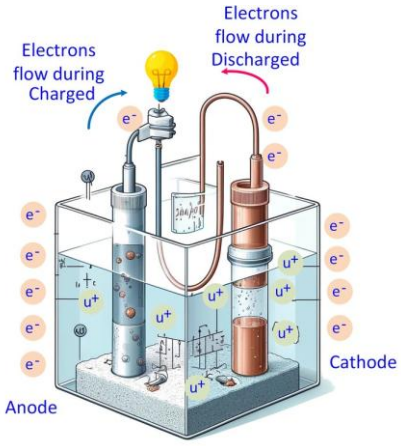

Figure 2. The process of producing Li-ion battery with silicon anode**.**

During charging, electrons flow from the power source to the anode, with positive ions (u^+) moving towards the anode in the electrolyte. During discharging, electrons flow from the anode to the cathode through the external circuit, powering a bulb, while positive ions move towards the cathode in the electrolyte.

The blue arrow shows electron flow during charging, and the red arrow shows electron flow during discharging. The labels e^- and u^+ denote electrons and positive ions, respectively. Charging involves an external energy source forcing electrons to the anode, causing reduction reactions, while discharging involves electrons flowing naturally from anode to cathode, causing oxidation at the anode and reduction at the cathode. This setup demonstrates the basic principles of converting chemical energy to electrical energy and vice versa, as seen in batteries. The active material, NMC811, performs the main electrochemical reactions. Carbon black enhances conductivity, while the binder holds the components together.

4.2 EIS Mathematical Modeling

Electrochemical Impedance Spectroscopy (EIS) is a method used to determine resistance (R), capacitance (C), and inductance (L) by observing the current response to an applied AC voltage in an electrochemical cell. IES analysis can be conducted by considering:

$$Z(\omega) = Z_0 \cos\theta + Z_0 \sin\theta\, j \quad (1)$$

where $Z'_{real} = Z_0 \cos\theta$ (R) and $Z''_{real} = Z_0 \sin\theta$ (C and L).

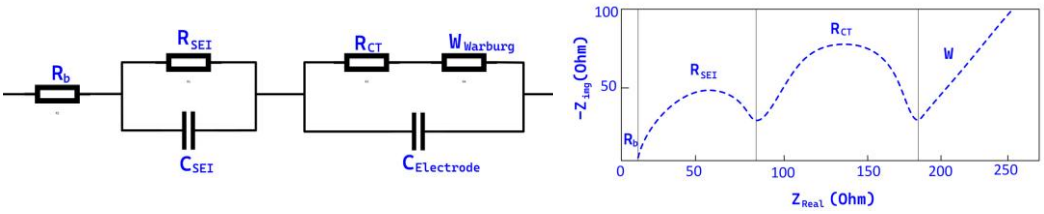

(a) Li-ion circuit modeling (b) EIS analysis diagram

Figure 3. EIS modeling [24].

Figure 3.a is the simplified equivalent circuit of a lithium battery and Figure 3.b. is the EIS graph to analyze the performance of the proposed method, where R_b is the bulk resistance of the cell, R_{SEI} and C_{SEI} are the resistance and capacitance of the interfacial layer, R_{CT} and $C_{electrode}$ are the charge-transfer resistance, and double layer capacitance, and W is the diffusional effect of Li-ion battery on the host material. The Nyquist plot provides key insights into lithium-ion batteries' characteristics. The initial x-axis intercept, Rb, reflects the total resistance of the electrolyte, separator, and electrodes, indicating the state of health. The first semicircle, RSEI, corresponds to the interfacial layer formation on the electrode, useful for analyzing the SEI layer formed from electrolyte decomposition and observing polymeric gel-like films in nano-sized electrodes through EIS. The second semicircle, Rct, relates to the electrochemical reaction kinetics, influenced by

factors like surface coating and particle size, representing the faradic charge-transfer resistance to elucidate the reaction mechanism and temperature-dependent traits. Finally, the Warburg impedance, shown as the last straight line, is associated with lithium-ion diffusion.

4.3. Battery Implementation to PV System Design

The battery produced in this study is integrated with a PV system. Figure 4 shows the design for charging lithium-ion with a silicon anode, and the load considered is the LED lamp. This section aims to show the feasibility of integrating a silicon anode battery with a PV system; hence, the design is kept simple with only one load, as shown in Figure 4. The Mathematical Modeling for a PV system with a silicon anode lithium-ion battery is similar to traditional systems but accounts for higher energy densities and efficiencies. Energi density calculation is given by:

$$\text{Energy Density } \left(\frac{\text{Wh}}{\text{L}}\right) = \frac{\text{Battery Capacity (Ah)} \times \text{Voltage(V)}}{\text{Battery Volume (L)}}, \quad (2)$$

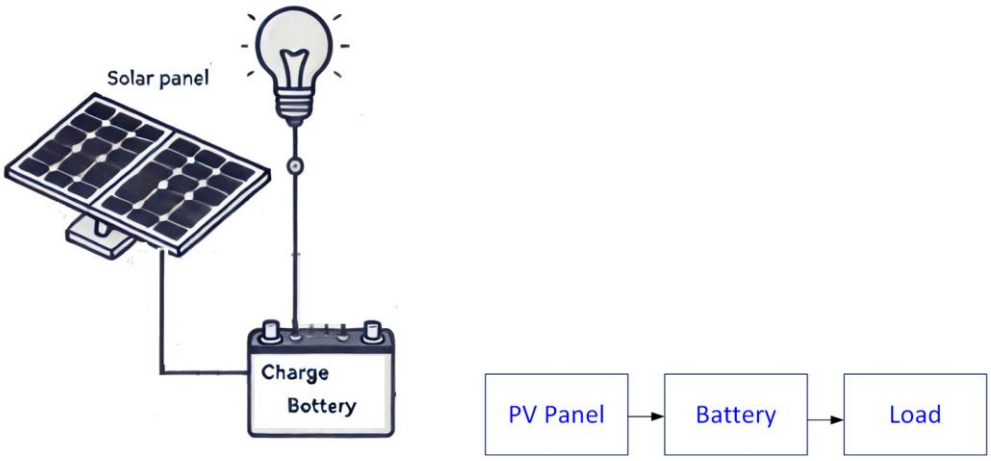

Figure 4. The PV charged battery setting in this study**.**

Energy efficiency in batteries is a measure of how effectively the battery converts input energy during charging into usable output energy during discharging. To calculate energy efficiency from the graph, it is necessary to determine the areas under the charge and discharge curves, as these areas represent the energy involved in each process. The charge/efficiency (η) or energy efficiency is given by:

$$\eta = \left(\frac{\text{Energy Out}}{\text{Energy In}}\right) \times 100\%, \quad (3)$$

while battery's cycle life is:

$$\text{Cycle Life} = \frac{\text{Total Number of Cycles}}{\text{Daily Cycles}}, \quad (4)$$

and Coulumbic Efficiency is:

$$\text{Coulombic Efficiency (\%)} = \frac{\text{Discharge Capacity}}{\text{Charge Capacity}} \times 100, \quad (5)$$

5. EXPERIMENT AND ANALYSIS

The experiment is conducted to show the effectiveness of the proposed method. The experimental steps is to ensure that the integration is successful and that the performance of the battery is thoroughly evaluated under real-world conditions.

5.1 Silicon Extraction from Fly Ash Waste

The fly ash taken from combustion waste of PT Semen Baturaja (Cement Manufacturing Company) is given in Figure 6.a and the extraced silica is given in Figure 6.b from the process illustrated in Figure 1, and the complete chemical component of fly as is given in Table 1.

(a) Fly ash (b) Silica

Figure 5. Fly ash and extracted silica**.**

Table 1. Chemical components extracted from fly ash

Component	Fly ash (%)	Extracted silica (%)
SiO_2	49.21	93.52
Al_2O_3	16.22	1.14
Fe_2O_3	5.49	1.17
K_2O	0.50	0.06
CaO	7.37	0.93
MgO	1.72	1.08

5.2 Battery Performance Analysis

The objective of this experiment is to thoroughly understand the battery's behavior, determine its capacity, evaluate its charge and discharge efficiency, analyze its cycle life, assess the impact of various operating conditions such as temperature and load, and IES analysis. Figure 6 are the battery produced in this study where Figure 6.a is 12 batteries pack, and figure 6.b is 3 batteries connected in series and paralel. Cycle life testing is another critical part of the experiment, where the battery is subjected to repeated charge and discharge cycles at a consistent current rate, such as C/2. Over multiple cycles, typically around 100, the battery's capacity, voltage profiles, and efficiency are closely monitored to assess performance degradation. Data

collected from these cycles helps determine the battery's capacity retention and degradation rate, providing valuable information about its long-term durability.

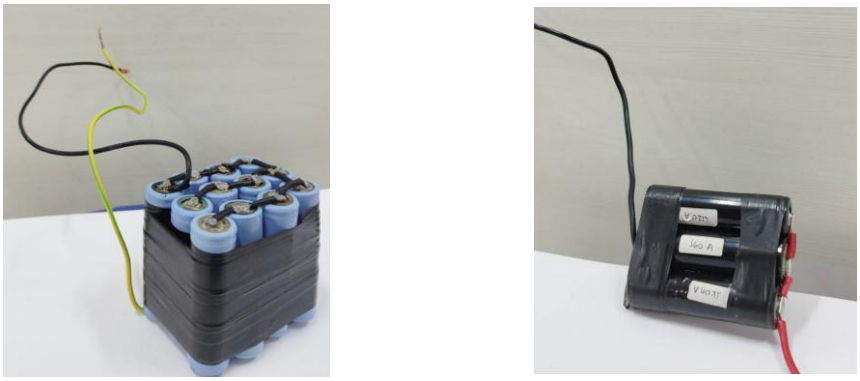

(a) (b)

Figure 6. The silicon anode battery produced in this study**.**

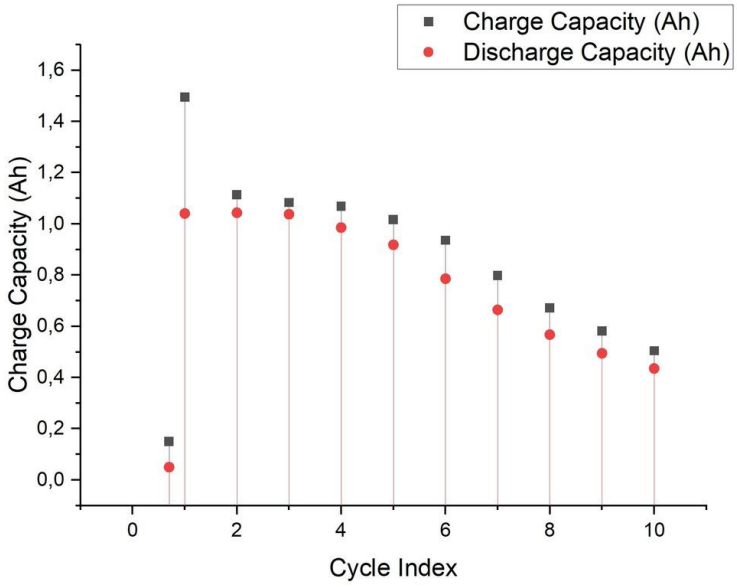

Figure 7. Charge and discharge cycle**.**

Figure 7 depicts the charge and discharge capacities of a lithium-ion battery over multiple cycles. The x-axis represents the cycle index, indicating the number of charge-discharge cycles the battery has undergone, while the y-axis represents the charge capacity in ampere-hours (Ah). Two sets of data are plotted: charge capacity (represented by black squares) and discharge capacity (represented by red circles). The charge capacity begins at approximately 1.5 Ah in the initial cycle, indicating the maximum amount of charge the battery can hold. However, there is a significant drop in capacity after the first cycle, stabilizing around 1.0 Ah for several subsequent cycles. Over time, the charge capacity gradually decreases, reaching about 0.7 Ah by

the 10th cycle. This decline suggests that the battery's ability to accept and store charge diminishes with repeated cycling, likely due to degradation mechanisms such as the formation of a solid electrolyte interphase (SEI) layer or structural changes in the silicon anode.

The discharge capacity, while initially close to the charge capacity, is consistently lower. Starting at around 1.0 Ah in the first cycle, it too drops significantly after the first cycle and continues to decrease steadily. By the 10th cycle, the discharge capacity falls to approximately 0.5 Ah. The consistent difference between the charge and discharge capacities indicates inefficiencies and energy losses during the charge-discharge process. The Coulombic and Energy efficiency of the proposed battery is given in Table 2, which measures the efficiency of charge transfer within the battery and typically decreases over time.

Table 2. Battery performance recapitulation

Cycle Index	Charge Capacity (Ah)	Discharge Capacity (Ah)	Coulombic Efficiency (%)	Energy Charge (Wh)	Energy Discharge (Wh)	Energy Efficiency (%)
1	1.5	1	66.67	5.7	3.6	63.16
2	1.2	1	83.33	4.56	3.6	78.95
3	1.1	0.9	81.82	4.18	3.24	77.51
4	1	0.85	85	3.8	3.06	80.53
5	1	0.8	80	3.8	2.88	75.79
6	0.9	0.75	83.33	3.42	2.7	78.95
7	0.8	0.65	81.25	3.04	2.34	76.97
8	0.75	0.6	80	2.85	2.16	75.79
9	0.7	0.55	78.57	2.66	1.98	74.44
10	0.7	0.5	71.43	2.66	1.8	67.67

Energy charge and discharge values are calculated based on assumed average voltages of 3.8V for charging and 3.6V for discharging. The energy charge starts at 5.7 Wh and drops to 2.66 Wh, while the energy discharge starts at 3.6 Wh and decreases to 1.8 Wh over ten cycles. Energy efficiency, the ratio of energy discharge to energy charge, starts at 63.16%, peaks at 80.53%, and declines to 67.67%, reflecting similar trends seen in Coulombic efficiency.

Figure 8 shows the distinct voltage plateau regions, particularly around 4.0V, which correspond to the intercalation of lithium ions into the silicon anode. The charge curve starts at around 2.4V and rises to approximately 4.2V as capacity increases. Conversely, the discharge curve begins at 4.2V and decreases, with a steep drop near the end indicating the battery's capacity limit. Figure 8 gives the high capacity and stable voltage plateaus of a lithium-ion battery with a silicon anode, while also pointing out areas for optimization such as the steep voltage drop at the end of discharge and voltage hysteresis.

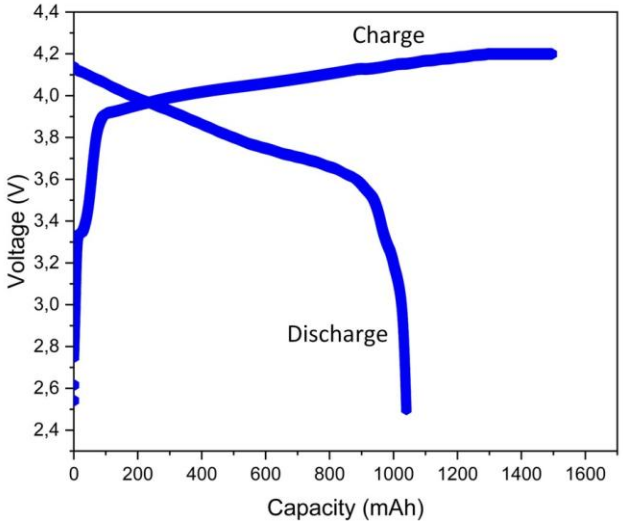

Figure 8. Voltage and capacity features during charging and discharging**.**

The material samples in this study is subjected to sonification to disperse and breakdown break down agglomerates, and enhance chemical reactions, which is crucial in the preparation of materials for silicon anode lithium batteries. The duration of sonication can significantly impact the performance and properties of the silicon anode, influencing factors such as particle dispersion, size reduction, and structural integrity, and this study 60 and 120 minutes sonification was conduction and both compared with withoud sonification IES performance, given in Figure 9.

No Sonication leads to poorly dispersed, larger silicon particles with broader XRD peaks and lower intensity. The resulting anode has poor electrical contact, higher internal resistance, and suboptimal battery performance. Sonication 60 achieves better particle dispersion and size reduction, indicated by narrower and more intense XRD peaks. This improves the silicon anode's distribution, electrical contact, and reduces internal resistance, leading to enhanced battery capacity, cycle life, and rate capability without significant structural changes, and Sonication 120 further improves dispersion and reduces particle size, resulting in very sharp and intense XRD peaks. While this maximizes surface area and reactivity, it may also induce structural changes or defects in the silicon anode, potentially affecting mechanical stability and leading to capacity fade and reduced cycle life.

Figure 9 displays a Nyquist plot used in electrochemical impedance spectroscopy (EIS) to analyze the impedance characteristics of three different samples silicon anode battery with no sonficiation (TS), 60 mins sonification (S60) and 120 mins sonificatin (S120).

The TS sample exhibits the highest impedance values, with Z'' reaching up to 45 kΩ and Z' extending to about 55 kΩ. This high impedance suggests significant resistance and capacitive behavior, indicating that the TS sample might have substantial internal resistance or poor conductivity. The large semicircle observed in the high-frequency region of the Nyquist plot typically

corresponds to charge transfer resistance (R_ct), which is a measure of the difficulty of electron transfer at the electrode/electrolyte interface. The substantial R_ct in the TS sample suggests it may be less efficient for electrochemical applications due to high resistance and poor charge transfer properties.

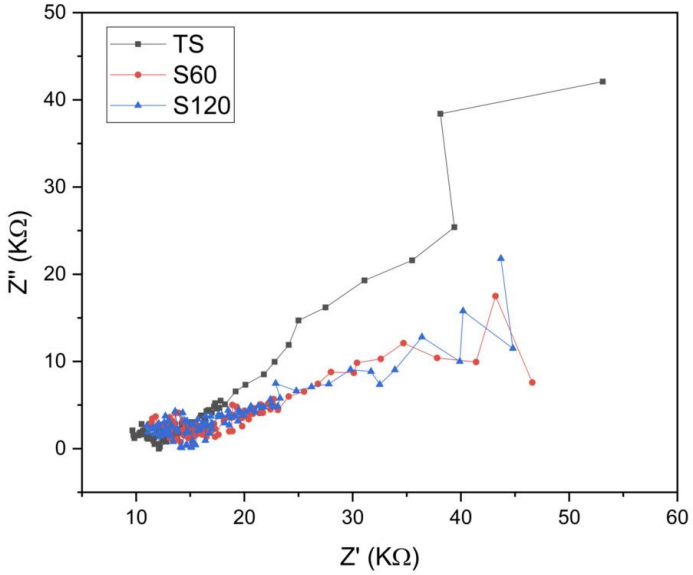

Figure 9. Charge and discharge cycle.

The S60 sample shows intermediate impedance values, with Z'' peaking around 15 kΩ and Z' values extending to approximately 45 kΩ. The smaller semicircle compared to the TS sample indicates lower charge transfer resistance, suggesting better conductivity and more efficient charge transfer at the electrode/electrolyte interface. The impedance characteristics of S60 imply that it has lower resistance and better electrochemical performance than TS, making it more suitable for applications that require moderate conductivity.

The S120 sample demonstrates the lowest impedance values among the three samples, with Z'' peaking around 10 kΩ and Z' values extending up to 40 kΩ. The smallest semicircle observed in the high-frequency region indicates the lowest charge transfer resistance, suggesting superior ionic and electronic conductivity. The low impedance values imply that the S120 sample has excellent charge transfer properties and minimal internal resistance, making it the most promising candidate for electrochemical applications, such as batteries and supercapacitors, where high efficiency and low resistance are crucial.

The differences in impedance characteristics among the TS, S60, and S120 samples can be attributed to variations in material composition, structure, and treatment processes. The high charge transfer resistance in the TS sample suggests that its material properties may hinder efficient electron transfer, whereas the lower charge transfer resistance in the S60 and S120 samples indicates better conductivity and more efficient electrochemical

behavior. The superior performance of the S120 sample, as evidenced by its low impedance and minimal charge transfer resistance, suggests that it has the best material properties for applications requiring high conductivity and low resistance; hence, this makes S120 the most suitable candidate for energy storage systems like batteries and supercapacitors.

5.3 Integration of Silicon Anode Battery into PV System

Integrating silicon anode batteries with PV panels, as shown in Figure 10 by connecting a mini PV panel with battery and a LED for load which reflects to Figure 4. This setup is used to test the performance of the PV system and the battery pack's storage capabilities. Table 3 shows the result of implementing proposed battery to a PV system where the irradiance, current, and voltage are recorded per-hour.. At 10:00, the voltage is 0.83V and the current is 0.03A, indicating low power generation. As the day progresses to 11:00, the voltage increases to 1.07V and the current rises to 0.43A, showing a significant increase in power generation. By 12:00, the voltage drops to 0.28V, while the current reaches 1.56A, suggesting that although the voltage is lower, the current is much higher, possibly due to different operating conditions or loads. At 13:00, the voltage is 0.34V and the current is 0.16A, which is a decrease from the earlier peak values.

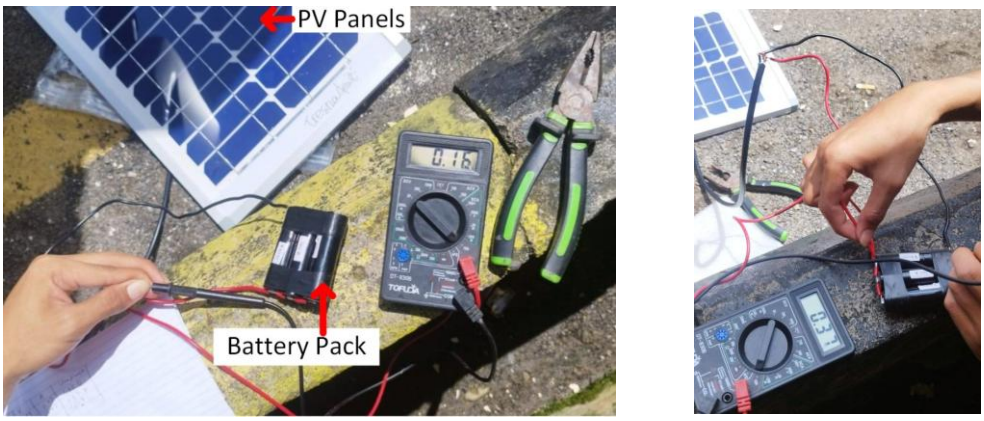

(a) (b)

Figure 10. Silicon anode integrated PV System.

Table 3. Implementation of silicon anode battery to PV System

NO	Time	Voltage (V)	Current (A)	Irradiance (W/m2)
1	10:00	0.83	0.03	638.6
2	11:00	1.07	0.43	1173.7
3	12:00	0.28	1.58	1181.3
4	13:00	0.34	0.16	1244.2

The irradiance values show a consistent increase from 638.6 W/m^2 at 10:00 to a peak of 1244.2 W/m^2 at 13:00. Typically, higher irradiance results

in higher power output from the PV system. However, the voltage does not show a direct proportional relationship with irradiance, indicating that factors such as PV cell characteristics, load conditions, and temperature effects may influence the results.

The integration of silicon-anode battery to PV panels is implemented in this study, where the silicon is extracted from fly ash. The experimental results show that the battery is working as a storage system for PV panels.

6. CONCLUSION

The integration of silicon-anode lithium-ion batteries with photovoltaic (PV) systems significantly enhances energy storage capabilities. The successful extraction of silicon from fly ash, increasing SiO2 content from 49.21% to 93.52%, demonstrates the potential for repurposing industrial waste into valuable battery components. The energy charge and discharge experiments reveal that silicon-anode batteries maintain a high energy efficiency, peaking at 80.53%, although it declines to 67.67% after ten cycles. Impedance spectroscopy tests show that the S120 sample has the lowest impedance values, indicating superior electrochemical performance and making it the most suitable for high-efficiency applications like batteries and supercapacitors. The PV system integration experiments illustrate that while increased irradiance generally boosts power output, other factors such as PV cell characteristics and load conditions also play critical roles. The data indicates that voltage and current do not always proportionally align with irradiance levels. The random forest model shows limitations in accurately predicting current values, highlighting the need for further refinement in predictive analytics. In summary, the integration of fly ash-derived silicon anodes in lithium-ion batteries with PV systems offers a sustainable and efficient solution for energy storage, addressing both environmental and technological challenges. This approach not only improves battery performance but also promotes the circular economy by converting waste into high-value products.

Acknowledgments

The authors would like to acknowledge the Renewable Energy Engineering Department, Politeknik Negeri Sriwijaya, and PPM Dit. APTV through Contract No. 55/SPK/D.D4/PPK.01.APTV/III/2024 for funding supports this Master's Thesis Research. The authors also would like to thank Politeknik Negeri Sriwijaya for the supporting academic atmosphere.

REFERENCES

[1] H. M. Yudha, T. Dewi, P. Risma, and Y. Oktarina, **Life Cycle Analysis for the Feasibility of Photovoltaic System Application in Indonesia**, in *IOP Conf. Series: Earth and Environmental Science*, vol. 124, 2018, doi: 10.1088/1755-1315/124/1/012005.

[2] T. Dewi, P. Risma, and Y. Oktarina, **A Review of Factors Affecting the Efficiency and Output of a PV system Applied in Tropical Climate**, in *IOP Conf. Series: Earth and Environmental Science*, vol. 258, 2019, doi: 10.1088/1755-1315/258/1/012039.

[3] A. Zullah, T. Dewi, and Rusdianasari, **Performance Analysis of Ship Mounting PV Panels Deployed in Sungsang Estuary and Bangka Strait, Indonesia**, Sinergi, vol. 28, no. 1, 2024, doi: http://dx.doi.org/10.22441/sinergi.2024.1.017.

[4] S. Polat and H. Sekerci, **The Determination of Optimal Operating Condition for an Off-Grid Hybrid Renewable Energy Based Micro-Grid: A Case Study in Izmir, Turkey**, EMITTER International Journal of Engineering Technology, vol. 9, no. 1, pp. 597-608, Mar. 2021, doi: 10.24003/emitter.v9i1.597.

[5] A. A. Sasmanto, T. Dewi, and Rusdianasari, **Eligibility Study on Floating Solar Panel Installation over Brackish Water in Sungsang, South Sumatra**, EMITTER International Journal of Engineering Technology, vol. 8, no. 1, pp. 514-523, Mar. 2020, doi: 10.24003/emitter.v8i1.514.

[6] B. P. A. Rohman, C. Hilman, E. Tridianto, and T. H. Ariwibowo, **Power Generation Forecasting of Dual-Axis Solar Tracked PV System Based on Averaging and Simple Weighting Ensemble Neural Networks**, EMITTER International Journal of Engineering Technology, vol. 6, no. 2, pp. 341-351, Dec. 2018, doi: 10.24003/emitter.v6i2.341.

[7] T. B. Sitorus, Z. Lubis, F. Ariani, and F. Sembiring, **Study on Thermoelectric Cooler Driven by Solar Energy in Medan City**, EMITTER International Journal of Engineering Technology, vol. 6, no. 2, pp. 303-311, Dec. 2018, doi: 10.24003/emitter.v6i2.303.

[8] Y. Oktarina, Z. Nawawi, B. Y. Suprapto and T. Dewi, **Digitized Smart Solar Powered Agriculture Implementation in Palembang, South Sumatra**, in *Proc. 2023 10th Int. Conf. on Electrical Engineering, Computer Science and Informatics (EECSI)*, Palembang, Indonesia, 2023, pp. 60-65, doi: 10.1109/EECSI59885.2023.10295805.

[9] Y. Mases, T. Dewi, and Rusdianasari, **Solar Radiation Effect on Solar Powered Pump Performance of an Automatic Sprinkler System**, in *Proc. 2021 Int. Conf. on Electrical and Information Technology (IEIT)*, 2021, pp. 246-250, doi: 10.1109/IEIT53149.2021.9587360

[10] P. P. Putra, T. Dewi, and Rusdianasari, **MPPT Implementation for Solar-powered Watering System Performance Enhancement**, Technology Reports of Kansai University, vol. 63, no. 1, pp. 6919-6931, 2021. ISSN: 04532198.

[11] T. Sujati, T. Dewi, and Rusdianasari, **Charging System Design of a Solar Powered Mobile Manipulator**, in *Proc. 2021 Int. Conf. on Electrical and Information Technology (IEIT)*, 2021, pp. 179-184, doi: 10.1109/IEIT53149.2021.9587401

[12] F. Septiarini, T. Dewi, and Rusdianasari, **Design of a solar-powered mobile manipulator using fuzzy logic controller of agriculture**

application, Int. J. Comput. Vis. Robot., vol. 12, no. 5, pp. 506-531, 2022, doi: 10.1504/IJCVR.2022.125356.
[13] B. Dunn, H. Kamath, and J.-M. Tarascon, **Electrical energy storage for the grid: a battery of choices**, Science, vol. 334, pp. 928-935, 2011.
[14] P. J. Hall and E. J. Bain, **Energy-storage technologies and electricity generation**, Energy Policy, vol. 36, pp. 4352-4355, 2008.
[15] N. Nitta, F. Wu, J. T. Lee, and G. Yushin, **Li-ion battery materials: present and future**, Materials Today, vol. 18, no. 5, pp. 252-264, 2015.
[16] D. S. Jung et al., **Recycling rice husks for high-capacity lithium battery anodes**, *Proceedings of the National Academy of Sciences of the United States of America*, vol. 110, pp. 12229–12234, 2013.
[17] N. Liu et al., **Rice husks as a sustainable source of nanostructured silicon for high performance Li-ion battery anodes**, Scientific Reports, vol. 3, p. 1919, 2013.
[18] Y. Jiang et al., **A sustainable route from fly ash to silicon nanorods for high performance lithium ion batteries**, Chemical Engineering Journal, vol. 330, pp. 1052–1059, 2017.
[19] N. Shigemoto, H. Hayashi, and K. Miyaura, **Selective formation of Na-X zeolite from coal fly ash by fusion with sodium hydroxide prior to hydrothermal reaction**, Journal of Materials Science, vol. 28, pp. 4781-4786, 1993, doi: 10.1007/BF00354621.
[20] S. S. Bukhari, J. Behin, H. Kazemian, and S. Rohani, **Conversion of coal fly ash to zeolite utilizing microwave and ultrasound energies: A review**, Fuel, vol. 140, pp. 250-266, 2015, doi: 10.1016/j.fuel.2014.09.077.
[21] K. Burnard and S. Bhattacharya, **Power generation from coal,** IEA Energy Papers, 2011, doi: 10.1787/5kg3n27pxf0n-en.
[22] N. Chandra, P. Sharma, G. L. Pashkov, E. N. Voskresenskaya, S. S. Amritphale, and N. S. Baghel, **Coal fly ash utilization: Low temperature sintering of wall tiles**, Waste Management, vol. 28, pp. 1993-2002, 2008, doi: 10.1016/j.wasman.2007.06.009.
[23] J.-Y. Li et al., **Research progress regarding Si-based anode materials towards practical application in high energy density Li-ion batteries**, Materials Chemistry Frontiers, vol. 1, pp. 1691–1708, 2017.
[24] W. Choi, H.-C. Shin, J. M. Kim, J.-Y. Choi, and W.-S. Yoon, **Modeling and Applications of Electrochemical Impedance Spectroscopy (EIS) for Lithium-ion Batteries**, J. Electrochem. Sci. Technol., vol. 11, no. 1, pp. 1-13, 2020, doi: 10.33961/jecst.2019.00528.